

## Magnetoresistance effect and interlayer exchange coupling in epitaxial Fe/Au(100) and Fe/Au(111) multilayers

K. Shintaku,\* Y. Daitoh, and T. Shinjo

*Institute for Chemical Research, Kyoto University, Uji, Kyoto-fu 611, Japan*

(Received 16 November 1992)

Single-crystal-like Fe/Au(100) and polycrystalline Fe/Au(111) multilayers were prepared by ultrahigh-vacuum deposition. In the Fe/Au(100) system, a distinct oscillation in the magnetoresistance (MR) ratio in accordance with the changes of interlayer exchange coupling was observed at room temperature as a function of Au-spacer-layer thickness. In the Fe/Au(111) system, an antiferromagnetic coupling was also confirmed. Flatness of interfaces and well-controlled spacer-layer thicknesses are crucial factors to ensure observation of the MR-oscillation effect.

The giant-magnetoresistance (GMR) effect and its oscillation as a function of nonmagnetic spacer-layer thickness have attracted much attention as a peculiar phenomenon in metallic multilayers; this is not only because of the primary importance of the subject of physical science but also because of potential technological applications.<sup>1,2</sup> An antiferromagnetic (AF) interlayer exchange coupling of magnetic layers through nonmagnetic spacer layers is regarded as one of the origins of the GMR effect. However, since the mechanism has not been fully understood, well-controlled single-crystal-like multilayer films are necessary to get reliable and comprehensive data.

Fe layers are epitaxially grown on Au substrates because there is very little difference in the atomic distances of their metal structures.<sup>3</sup> Therefore, we can obtain single-crystal-like Fe/Au films with high quality as model materials to study interlayer exchange coupling of magnetic layers spaced by a nonmagnetic layer. Oscillatory magnetic exchange coupling as a function of Au-spacer-layer thickness was reported in Fe/Au/Fe trilayer films with the use of ferromagnetic resonance<sup>4</sup> (FMR) measurements and in Fe/Au/Fe trilayer films with wedge-shaped Au layers with the use of the surface magneto-optical Kerr effect (SMOKE).<sup>5</sup> However, oscillation in the magnetoresistance (MR) was not reported. In particular, for polycrystalline Fe/Au(111) multilayers prepared by magnetron sputter deposition, no interlayer exchange coupling is observed.<sup>6</sup> We have observed clear oscillations in both the MR and exchange coupling in single-crystal-like Fe/Au(100) multilayers prepared with ultrahigh-vacuum (UHV) deposition. Moreover, the shape of the oscillation is different from ones reported in many systems so far.

The samples were prepared by alternate deposition in UHV conditions with electron-gun heating. The pressure reached  $(1-4) \times 10^{-9}$  torr before deposition and remained at  $(5-9) \times 10^{-9}$  torr during deposition. GaAs(100) single crystals chemically etched with a conventional method ( $\text{H}_2\text{SO}_4:\text{H}_2\text{O}_2:\text{H}_2\text{O}=3:1:1$ ) (Ref. 7) and glasses were used as substrates in order to change crystallographic orientations and crystallinity. The deposition rate was 0.2–0.3 Å/sec for Au and 0.1–0.2 Å/sec for Fe. A typical film-growth process is as follows. After

heating substrates at 300°C for more than an hour; 470-Å-thick Au were evaporated on the substrates at the substrate temperature ( $T_s$ ) of 200°C. Fe/Au multilayers were grown with 20 repetitions on buffer layers at  $T_s=50^\circ\text{C}$ . 47-Å-thick Au protection layers covered the multilayers. Since the quartz-crystal oscillator as a thickness monitor *in situ* cannot resolve the film thicknesses less than 1 Å, a geometrical condition of the substrates' holder in the preparation chamber was utilized to prepare the samples by controlling the film thickness less than 1 Å.

The flatness of the film surfaces during film growth was confirmed by reflection high-energy electron-diffraction (RHEED) patterns. The structures of the prepared samples were investigated by x-ray diffraction (XRD) using the  $\theta$ - $2\theta$  scan method with Cu  $K\alpha$  radiation. A cross-sectional image of the film was observed with a transmission-electron microscope (TEM).

The magnetization curves were measured with a vibrating-sample magnetometer (VSM). The MR measurements were carried out by a conventional four-terminal method. In all cases, the magnetic fields were applied along the easy axis of Fe[100] in the film plane. In MR measurements, the applied fields were perpendicular to the current direction. All measurements were performed at room temperature (RT).

Single-crystal-like growth of Au and Fe layers on GaAs(100) substrates was confirmed by RHEED observation. The RHEED patterns for Au buffer layers on GaAs(100) substrates change from spots to streaklike patterns around 150 Å thick and become clear streaks thicker than 350 Å. When Fe layers are grown on Au layers, the RHEED patterns become slightly spotlike until 4 Å thick, but do not change after that. On the contrary, the RHEED patterns for Au layers on Fe layers revert to clear streaks for 10 Å thick. Figure 1 shows examples of RHEED patterns. The incident beam is parallel to GaAs[110]. The streak patterns become neater as the number of bilayer repetitions increases, which indicates that film flatness becomes better with film growth. On the other hand, for the samples on glass substrates, RHEED patterns were rings which indicate the samples being polycrystalline.

From XRD measurements, a number of small-angle

diffraction peaks and middle-angle satellite peaks were observed for the samples on both substrates, indicating epitaxial growth with controlled periodicity. Figure 2 shows an XRD pattern of the sample of  $\text{Au}(470 \text{ \AA})/[\text{Fe}(9.6 \text{ \AA})/\text{Au}(66 \text{ \AA})]_{19}/\text{Fe}(9.6 \text{ \AA})/\text{Au}(47 \text{ \AA})$  on GaAs and a glass substrate. It is worth noticing that the eighth peak in the small-angle region disappears for the sample on the GaAs substrate. This indicates that an ideal multilayer with a thickness ratio of  $\text{Fe}:\text{Au} \approx 1:7$  is grown. The film thicknesses of the Fe and Au layers were estimated from the spacings of satellite peaks. The orientational relationships of Fe layers and Au layers on GaAs substrates determined from XRD and RHEED observations are  $[\text{GaAs}(001)] \parallel [\text{fcc Au}(001)] \parallel [\text{bcc Fe}(001)]$  in the stacking direction and  $[\text{GaAs}(110)] \parallel [\text{fcc Au}(110)] \parallel \text{bcc Fe}(100)$  in the film plane. On the other hand, for the samples on glass substrates, the orientations are  $[\text{fcc Au}(111)] \parallel [\text{bcc Fe}(110)]$  in the stacking direction and polycrystalline in the film plane [see Ref. 8 regarding the

XRD study on  $\text{Fe}/\text{Au}(100)$  multilayers].

TEM images of the cross section of  $\text{Au}(470 \text{ \AA})/[\text{Fe}(9.6 \text{ \AA})/\text{Au}(28 \text{ \AA})]_{19}/\text{Fe}(9.6 \text{ \AA})/\text{Au}(47 \text{ \AA})$  on GaAs and glass substrates are shown in Fig. 3. Figure 3(a) indicates that the sample on the GaAs substrate has flat interfaces all over the sample. On the other hand, the sample on the glass substrate as shown in Fig. 3(b) has fairly rough interfaces compared with that on the GaAs substrate.

The difference in film structure on both substrates affects interlayer exchange coupling and MR. Figure 4 shows the magnetization curves and MR curves for  $\text{Fe}/\text{Au}(100)$  films on GaAs substrates exhibiting a ferromagnetic (F) and an AF interlayer exchange coupling. The role of the Au buffer layer is crucial in the  $\text{Fe}/\text{Au}(100)$  system. Without Au buffer layers of adequate thickness more than  $400 \text{ \AA}$ , which is consistent with the results of RHEED observation, the AF state in  $\text{Fe}/\text{Au}(100)$  multilayers on GaAs substrates as shown in Fig. 5(b) is not realized, that is, the remanent magnetization ( $M_r/M_s$ ) is relatively large and the saturation fields ( $H_s$ ) is small. As a result, the MR effect is small. Thus, film flatness is necessary to get AF coupling for the samples on GaAs substrates. The MR change at RT in Fig. 4(d) is fairly large considering the rather thick Au buffer layer of  $470 \text{ \AA}$ . Figure 5 shows the magnetization curves for  $\text{Fe}/\text{Au}(111)$  films on glass substrates exhibiting AF and F coupling. Figure 6 shows Au-spacer-layer depen-

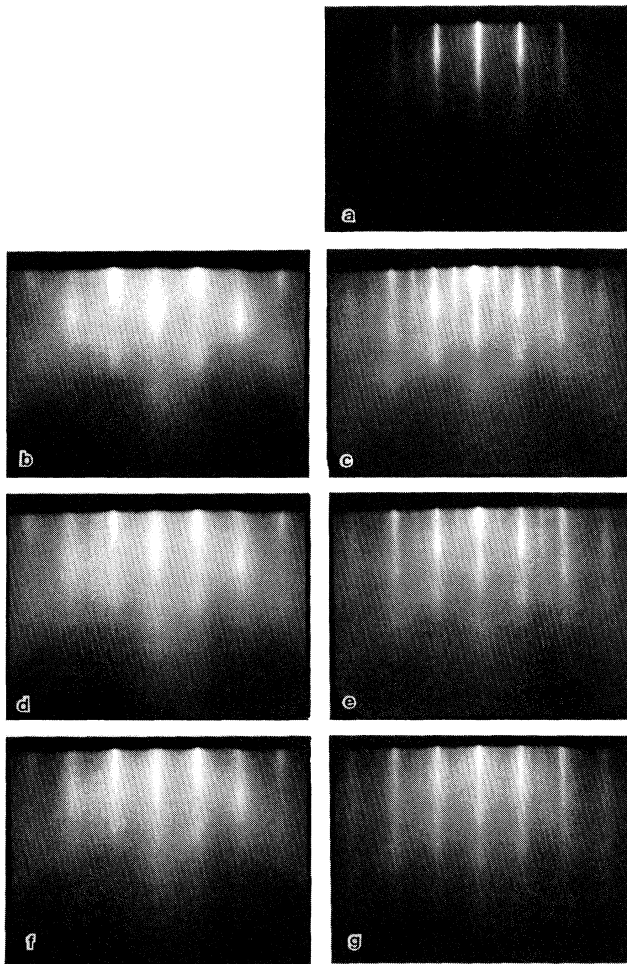


FIG. 1. RHEED patterns of  $\text{Au}(470 \text{ \AA})/[\text{Fe}(9.6 \text{ \AA})/\text{Au}(28 \text{ \AA})]_{19}/\text{Fe}(9.6 \text{ \AA})/\text{Au}(47 \text{ \AA})$  on GaAs substrate after depositing the (a) Au buffer layer of  $470 \text{ \AA}$ , (b) first Fe layer of  $470 \text{ \AA}$ , (c) first Au layer of  $28 \text{ \AA}$ , (d) tenth Fe layer of  $9.6 \text{ \AA}$ , (e) tenth Au layer of  $28 \text{ \AA}$  (f) 20th Fe layer of  $9.6 \text{ \AA}$ , and (g) 20th Au layer of  $28 \text{ \AA}$ .

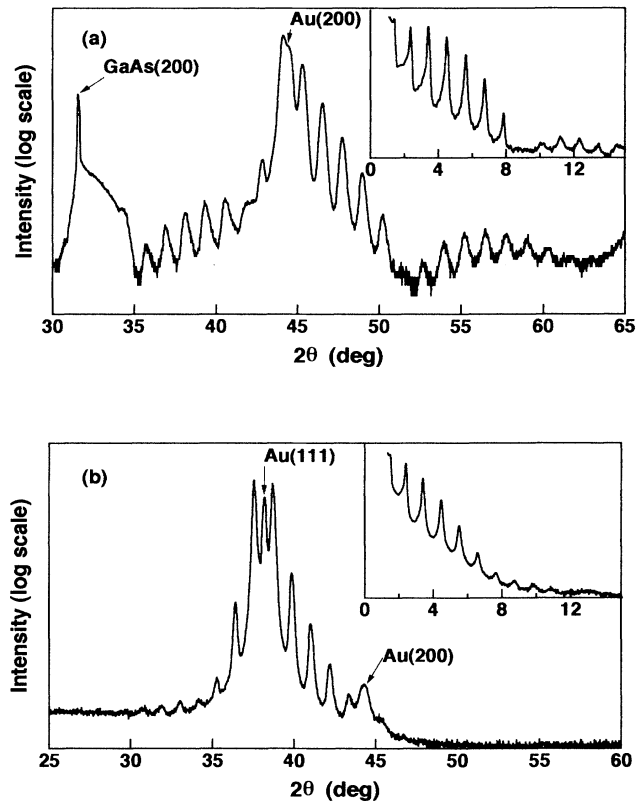


FIG. 2. XRD patterns of  $\text{GaAs}/\text{Au}(470 \text{ \AA})/[\text{Fe}(9.6 \text{ \AA})/\text{Au}(66 \text{ \AA})]_{19}/\text{Fe}(9.6 \text{ \AA})/\text{Au}(47 \text{ \AA})$  on the (a) GaAs substrate and (b) glass substrate. Inset: small-angle regions.

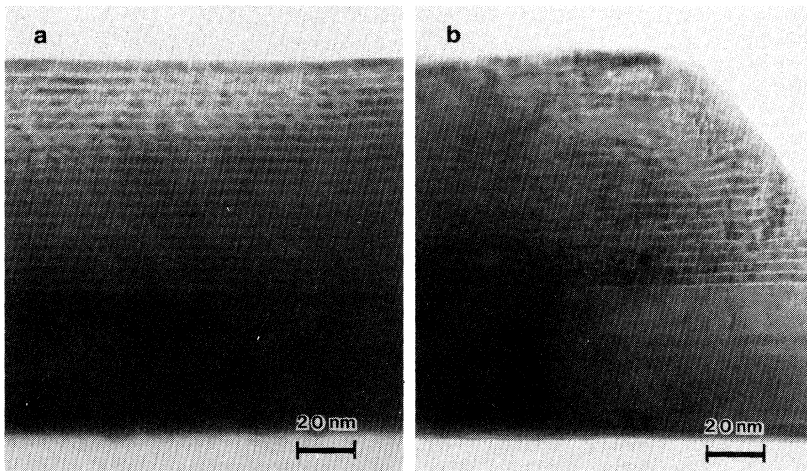


FIG. 3. Cross-sectional TEM images of Au(470 Å)/[Fe(9.6 Å)/Au(28 Å)]<sub>19</sub>/Fe(9.6 Å)/Au(47 Å) on the (a) GaAs substrate and (b) glass substrate.

dence of the MR ratio,  $M_r/M_s$ , and  $H_s$  for the samples with fixed Fe layers of 9.6 Å. The thickness of Au buffer layers is 470 Å for both substrates. The MR values are defined as  $\Delta\rho/\rho_s = \{\rho(H) - \rho(H=H_s)\} / \rho(H=H_s)$ , where  $\rho(H)$  is an electrical resistivity when the applied field is  $H$  Oe. The magnitude of  $\rho(H=H_s)$  is 5–7  $\mu\Omega$  cm and 6–9  $\mu\Omega$  cm for the samples on GaAs and glass substrates, respectively. For the samples on GaAs substrates, at least four maxima of the MR ratio are clearly observed and the three maxima at Au-spacer-layer thicknesses of 22, 33, and 47 Å are extremely sharp as shown in Fig. 6(a). The peak width of the MR ratio as a function of Au-spacer-layer thickness is about 1 Å. A slight difference in Au-spacer-layer thickness greatly affects MR values. The peak-to-peak intervals are not constant but seem to become gradually longer with increasing Au-spacer-layer thickness (11, 14, and 21 Å). In accordance with the MR oscillation, the magnetization

curve shows alternately F states and AF states. Oscillations of  $M_r/M_s$  and  $H_s$  accompany the MR ratio in Figs. 6(b) and 6(c). Thus, the AF coupling corresponds to the enhancement of the MR effect. The AF coupling energy  $J$  can be estimated by  $J = M_s t_{Fe} H_s / 4$ ,<sup>9</sup> where  $M_s$  is the saturation magnetization of Fe and  $t_{Fe}$  is the Fe layer thickness.  $M_s$  of Fe layers is suggested to be the same as bulk bcc Fe by conversion electron Mössbauer spectroscopy. The maximum  $H_s$  at a second peak of 22 Å yields  $J \approx 0.02$  erg/cm<sup>2</sup>, which is much smaller than for molecular-beam-epitaxy grown (100)bcc Fe/Cu(15 Å)/Fe ( $J \approx 0.1$  erg/cm<sup>2</sup>).<sup>10</sup>

From Figs. 6(b) and 6(c) it is expected, for the samples on GaAs substrates, that the first peak position is around the Au-spacer-layer thickness of 7 Å. It is, however, not until Au layers more than 10 Å are grown on Fe layers that RHEED patterns become clear streaks for the sample on GaAs substrates. Therefore, due to the imperfection of Au layers, F layers may couple with each other and MR oscillation and clear AF coupling are not observed for a Au-spacer-layer thickness less than 20 Å. The peak positions of  $M_r/M_s$  in Fig. 6(a) and  $H_s$  in Fig. 6(b) reasonably agree with the results of Fe/(wedge-shaped Au)/Fe trilayers in Ref. 5, but the details are not exactly the same. Shorter periods, which were predicted theoretically<sup>11,12</sup> and confirmed using an Fe/(wedge-shaped Au)/Fe(100) trilayer,<sup>5</sup> were not detected in the

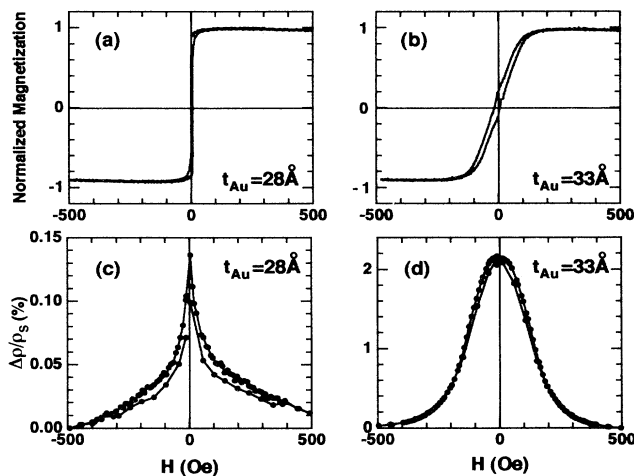


FIG. 4. Magnetization and MR curve of Au(470 Å)/[Fe(9.6 Å)/Au( $t_{Au}$  Å)]<sub>19</sub>/Fe(9.6 Å)/Au(47 Å) on the GaAs substrate with (a) and (b)  $t_{Au} = 28$  and (c) and (d)  $t_{Au} = 33$  Å at RT. The field is applied perpendicular to current direction in film plane.

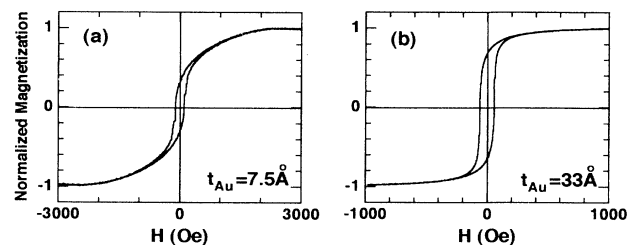


FIG. 5. Magnetization curve of Au(470 Å)/[Fe(9.6 Å)/Au( $t_{Au}$  Å)]<sub>19</sub>/Fe(9.6 Å)/Au(47 Å) on the glass substrate with (a)  $t_{Au} = 7.5$  Å and (b)  $t_{Au} = 33$  Å at RT.

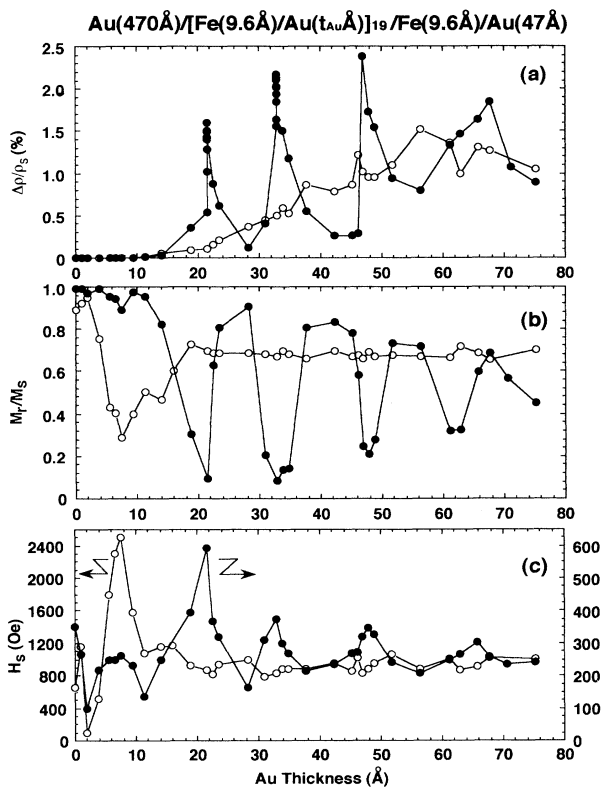


FIG. 6. Au-spacer-layer thickness dependence of the (a) MR ratio, (b)  $M_r/M_s$ , and (c)  $H_s$  of  $\text{Au}(470 \text{ \AA})/[\text{Fe}(9.6 \text{ \AA})/\text{Au}(t_{\text{Au}} \text{ \AA})]_{19}/\text{Fe}(9.6 \text{ \AA})/\text{Au}(47 \text{ \AA})$  on GaAs substrates [ $\bullet$ , single-crystal-like Fe/Au(100) multilayers] and glass substrates [ $\circ$ , polycrystalline Fe/Au(111) multilayers] at RT.  $\Delta\rho/\rho_s = [\rho(H) - \rho(H = H_s)]/\rho(H = H_s)$ .

present multilayer samples. This may be the difference between trilayers with wedge-shaped Au layers and multilayers. Oscillations of the MR effect were found using sputtered samples<sup>2</sup> and such a phenomenon was

confirmed extensively in many systems in the samples prepared by sputtering. However, to reproduce the oscillations in UHV grown samples was not very easy. It seems to be for the first time in multilayer samples that more than three peaks are clearly observed in the values of the MR ratio as a function of spacer-layer thickness. It is expected that the periods of oscillations depend on the crystallographic orientations and structure of interlayer materials as predicted by theoretical calculation.<sup>12</sup> A detailed analysis of the structure of Fe layers and Au layers is in progress.

For the samples on glass substrates, on the other hand,  $M_r/M_s$  and  $H_s$  have one peak around the Au-spacer-layer thickness of 7 Å, whose magnetization curve certainly shows AF coupling type [Fig. 5(a)]. The MR ratio, however, does not oscillate as a function of Au-spacer-layer thickness and has only a broad maximum around 55 Å. The maximum  $J$  is estimated to be about 0.1 erg/cm<sup>2</sup> at an  $H_s$  peak of 7.5 Å, which is almost the same as that of the sputtered Fe(15 Å)/Cu(15 Å) multilayer.<sup>10</sup>

The difference between the samples on GaAs substrates and glass substrates is regarded as being partly due to film qualities such as crystallinity and flatness of interfaces, and partly due to crystallographic orientations. The high-quality samples with fcc Au(111) orientations are necessary to study this in further detail.

In summary, clear oscillations in the MR effect and interlayer exchange coupling are observed for single-crystal-like Fe/Au(100) multilayers on GaAs substrates prepared by UHV deposition. In the case of the Fe/Au(100) system, a well-controlled Au-spacer-layer thickness and flatness of interfaces are crucial to observe the oscillation in the MR effect. The AF exchange coupling in polycrystalline Fe/Au(111) multilayers is also confirmed.

This work was supported by Grant-in-Aid for Scientific Research on Priority Areas (No. 02254103) from the Ministry of Education, Science and Culture, Japan.

\*Present address: Advanced Thin Film Research Labs., Tokyo Research Center, TEIJIN Ltd., 4-3-2 Asahigaoka, Hino, Tokyo 191, Japan.

<sup>1</sup>M. N. Baibich, J. M. Broto, A. Fert, F. Nguyen Van Dau, F. Petroff, P. Eitenne, G. Creuzet, A. Friederich, and J. Chazelas, *Phys. Rev. Lett.* **61**, 2472 (1988).

<sup>2</sup>S. S. Parkin, N. More, and K. P. Roche, *Phys. Rev. Lett.* **64**, 2304 (1990).

<sup>3</sup>T. Okuyama, *Jpn. J. Appl. Phys.* **30**, 2053 (1991).

<sup>4</sup>Z. Celinski and B. Heinrich, *J. Magn. Magn. Mater.* **99**, L25 (1991).

<sup>5</sup>A. Fuß, S. Demokritov, P. Grünberg, and W. Zinn, *J. Magn. Magn. Mater.* **103**, L221 (1992).

<sup>6</sup>S. S. Parkin, *Phys. Rev. Lett.* **67**, 3598 (1991).

<sup>7</sup>J. S. Vermaak, L. W. Snyman, and F. D. Auret, *J. Cryst. Growth* **42**, 132 (1977).

<sup>8</sup>N. Nakayama, T. Okuyama, and T. Shinjo, *J. Phys.: Condens. Matter* **5**, 1173 (1993).

<sup>9</sup>A. Barthélemy, A. Fert, M. N. Baibich, S. Hadjoudi, F. Petroff, P. Eitenne, R. Cabanel, S. Lequien, F. Nguyen Van Dau, and G. Creuzet, *J. Appl. Phys.* **67**, 5908 (1990).

<sup>10</sup>M. T. Johnson, S. T. Purcell, N. W. E. McGee, R. Cochoorn, J. aan de Stegge, and W. Hoving, *Phys. Rev. Lett.* **68**, 2688 (1992).

<sup>11</sup>F. Petroff, A. Barthélemy, D. H. Mosca, D. K. Lottis, A. Fert, P. A. Schroeder, W. P. Pratt, Jr., R. Loloee, and S. Lequien, *Phys. Rev. B* **44**, 5355 (1991).

<sup>12</sup>P. Bruno and C. Chappert, *Phys. Rev. B* **46**, 261 (1992).

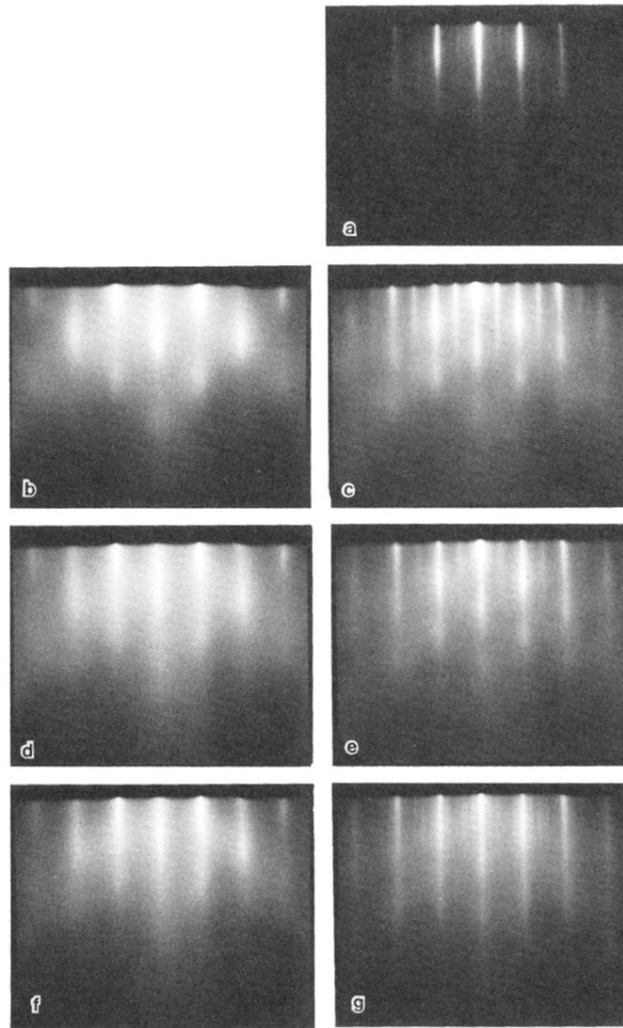


FIG. 1. RHEED patterns of Au(470 Å)/[Fe(9.6 Å)/Au(28 Å)]<sub>10</sub>/Fe(9.6 Å)/Au(47 Å) on GaAs substrate after depositing the (a) Au buffer layer of 470 Å, (b) first Fe layer of 9.6 Å, (c) first Au layer of 28 Å, (d) tenth Fe layer of 9.6 Å, (e) tenth Au layer of 28 Å (f) 20th Fe layer of 9.6 Å, and (g) 20th Au layer of 28 Å.

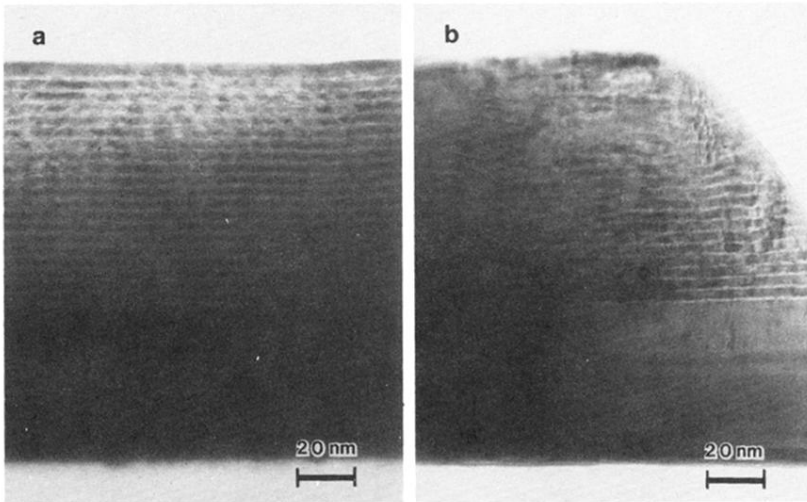


FIG. 3. Cross-sectional TEM images of  $\text{Au}(470 \text{ \AA})/[\text{Fe}(9.6 \text{ \AA})/\text{Au}(28 \text{ \AA})]_{19}/\text{Fe}(9.6 \text{ \AA})/\text{Au}(47 \text{ \AA})$  on the (a) GaAs substrate and (b) glass substrate.